EDDY FORMATION BEHIND A COASTAL CAPE BY TRANSIENT LONGSHORE WINDSTRESS (NUMERICAL EXPERIMENTS)

Zhurbas Victor, Shirshov Institute of Oceanology, Russia
Kuzmina Natalia, Shirshov Institute of Oceanology, Russia
Lyzhkov Dmitry, Shirshov Institute of Oceanology, Russia

zhurbas@ocean.ru

It is shown that the process of eddy formation behind a coastal cape-like obstacle essentially depends on the method of generating the longshore current. Numerical simulations of the flow around a cape generated by transient longshore wind reveal different modes of eddy formation in rotating stratified environment depending on dimensionless parameters such as the Burger and Kibel-Rossby numbers, Bu and Ro, respectively. At Ro<0.6 depending on the magnitude of Bu either trapped anticyclonic or cyclonic eddy at Bu<0.2 or periodic eddy shedding at Bu>0.2 is realized. The eddies are weakened and stretched along the coastline at 0.4–0.6<Ro<1.4 and ultimately disappear at Ro>1.4.

Key words: leeward eddy shedding, numerical simulation, Burger and Kibel-Rossby numbers

I. INTRODUCTION

Leeward eddies are known to be commonly generated behind prominent headlands and coastal capes [2–7, 9,10]. These eddies play an important role in physical, biological, ecological and geological processes in the coastal zone, such as an enhancement of mixing, flow resistance and coastal shelf – open sea exchange, transport and dispersion of pollutants, nutrients and sediments, etc.

The process of eddy generation behind coastal cape-like obstacles in rotating stratified environment depends on a number dimensionless parameters such as the Kibel-Rossby, $\mathrm{Ro} = U / |fD|$, Burger, $\mathrm{Bu} = N^2H^2 / f^2D^2 = (R_{bc} / D)^2$, and Ekman, $\mathrm{E} = \nu / |fH^2|$, numbers as well as the geometric parameter H / D, where ν is the kinematic viscosity, either molecular or turbulent, U is the flow velocity, f is the Coriolis parameter, N is the buoyancy frequency, D is the length scale of the obstacle in the cross-shore direction, H is the water column thickness (sea depth) and $R_{bc} = NH / f$ is the baroclinic deformation radius [2]. It is typical that $H / D = \mathrm{O}(1)$ in laboratory experiments and $H / D = \mathrm{o}(1)$ in the coastal seas.

The dependence of leeward eddy formation modes on Burger number at small values of Kibel-Rossby and Ekman numbers ($\mathrm{Ro} < 0.16 << 1$, $\mathrm{E} = (0.3–1.5)10^{-3} << 1$) was studied by Boyer and Tao [2] in laboratory experiments when the flow past a cape-like obstacle in rotating stratified channel was imitated by translating the channel floor, to which the obstacle was fixed. The main finding was the occurrence of the eddy shedding mode at large Burger number, $\mathrm{Bu} > 0.5–1$, and the attached (trapped) eddy mode at smaller Burger number, $\mathrm{Bu} < 0.5$, both in the cases of a left- and right-side obstacle (facing downstream at $f > 0$); the left-side (right-side) obstacle generated cyclonic (anticyclonic) eddies.

Elkin and Zatsepin [5] recently reported laboratory experiments on leeward eddy formation at small Ekman number, $E << 1$, but moderate Kibel-Rossby number, $Ro \le 0.6 = O(1)$, when the flow past a cape-like obstacle in rotating stratified round basin was imitated by a change (either increase or decrease) of the angular velocity of basin's rotation provided that before the change the solid-body rotation state of fluid in the basin had been achieved. The main finding was the occurrence of the eddy shedding regime for leeward anticyclonic eddies only while the leeward cyclonic eddies remained attached (trapped). The selective shedding of leeward anticyclonic eddies alone was explained by an increasing effect of the Ekman transport in the bottom layer with the increase of Ro [5].

To our minds, the way the flow past the obstacle was imitated in laboratory experiments [2, 5] could exaggerate the effect of bottom friction on leeward eddy formation as applied to stratified environment, because it generated vertically uniform flow regardless of the presence of density stratification in water column. Meanwhile, it is typical for a stratified sea environment that the flow is baroclinic and its velocity largely decreases with depth in the pycnocline layer which makes the bottom friction inessential. The aim of this work is to numerically simulate baroclinic flow past coastal obstacle in rotating stratified media by a transient longshore windstress, and study in this way the leeward eddying in a wide range of Bu and Ro.

II. Model Setup

Numerical experiments were performed on the base of the Princeton Ocean Model [1]. A rounded basin of constant depth, $H = 40$m, was taken for the model domain. To imitate a coastal cape, the shoreline curve, $r(\varphi)$, was set in polar coordinates (r - radius, φ - angle) by

$$r(\varphi) = \begin{cases} R_0 - D\varphi / 2\pi, & 0 < \varphi < 2\pi \\ R_0 - D \le r \le R_0, & \varphi = 0 \end{cases}, \qquad (1)$$

where R_0 is the undisturbed radius of the basin, $D \le R_0$. In the numerical experiments we took $R_0 = 75\,\text{km}$ for $10\text{km} \le D \le 20\text{km}$ and $R_0 = 37.5\text{km}$ for $3\text{km} \le D < 10\text{km}$. The basin's geometry is illustrated in Fig. 1.

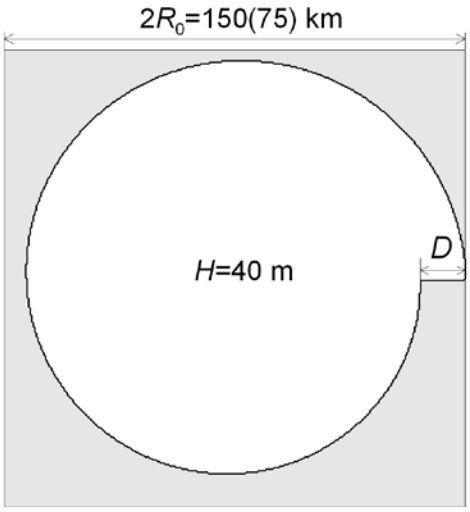

Fig. 1. The basin's geometry.

The finite-difference grid dimension is 301×301×25, i.e. there are 24 uniform layers in the vertical direction and the horizontal grid size is 0.5km at $10\text{km} \le D \le 20\text{km}$ and 0.25km at $3\text{km} \le D < 10\text{km}$. Thus, the size of cape-like obstacle is 12–40 times as large as the grid size, so the model is able to easily resolve the leeward eddy.

The initial stratification consists of two layers, each of 20m thick, with temperature of 20°C and 5°C in the top and bottom layers, respectively, and uniform salinity of 35 g/kg throughout whole water column. The baroclinic radius of deformation is calculated as $R_{bc} = (g^* H)^{1/2} / f$, where $g^* = g\Delta\rho / \rho_0 = 0.0286$ m/s^2 is the reduced gravity, $g = 9.81$ m/s^2, $\Delta\rho$ is the density jump between the layers, and $\rho_0 = 1000$kg/m^3 is the reference density. The value of R_{bc} varies in the range of $R_{bc} = 3.6$–21.4km, exceeding the grid size more than 7 times, which makes the model eddy-resolving.

To generate the longshore current, a transient "solid-body" tangential stress $\tau_\varphi(r,t)$ is applied to the basin's surface

$$\tau_\varphi(r,t) = \begin{cases} \tau_0 r / R_0, & 0 < t \le t_0 \\ 0, & t > t_0 \end{cases}, \quad \tau_r = 0. \tag{2}$$

In the main body of numerical experiments the surface stress value and duration are taken at $\tau_0 = 0.1$N/m^2 (which corresponds to 8 m/s of the 10m level wind velocity), and $t_0 = 1$day; the whole-basin gyring is counter-clockwise. In this way, we managed to create a fading longshore flow past the cape-like obstacle with the initial velocity in the range of $U =$ 0.15–0.55 m/s, where for definiteness as U was taken the maximum speed of the undisturbed flow before the obstacle at 10m depth and $t = t_0$.

In numerical experiments the change of dimensionless parameters Bu and Ro was achieved through variation of D and f, within the range of $D = 3$–20km and $|f| = (0.5$–$3.0)10^{-4}$ s^{-1}, respectively; the positive (negative) values of f corresponded to anticyclonic (cyclonic) leeward eddies. To avoid confusion, note that in the following figures, both cyclonic and anticyclonic eddies display clockwise rotation, but the pressure anomaly (not shown) has different sign (the anomaly is positive in anticyclones and negative in cyclones). The range of Bu and Ro change achieved in the numerical experiments is $\text{Ro} = 0.04$–4.5 and $\text{Bu} = 0.03$–50. In addition, the numerical experiments with large values of Burger and Kibel-Rossby numbers, $\text{Bu} > 2$ and $\text{Ro} > 1.6$, were reproduced at the same values of D and f but smaller τ_0 from the range of $\tau_0 = 0.0125$–0.1N/m^2, which conserved the old values of Bu but decreased Ro (due to the decrease of U). This has been done in order to determine the dependence of the leeward eddying mode on Ro. There was no sense to carry out the numerical experiments at a higher value of the windstress, $\tau_0 > 0.1$ N/m^2, in view of the possibility to achieve the state of fully developed upwelling/downwelling when the longshore flow detaches from the shoreline and becomes unstable, causing baroclinic eddies even if any coastal obstacles are missing [11].

III. RESULTS

By the definition of the dimensionless parameters, $\text{Bu} = (R_{bc} / D)^2 = g^* H / (fD)^2$ and $\text{Ro} = U / |fD|$, variations of D and/or f, which took place in the main body of numerical experiments, result in simultaneous increase/decrease of both Bu and Ro. The numerical experiments showed four modes of leeward eddy formation depending on the value of Bu and

Ro; three of the four modes can be regarded as the basic modes, and one as an intermediate mode. These modes are illustrated in Figs. 2–4.

At $\mathrm{Bu} < 0.2$ ($\mathrm{Ro} < 0.15$) an anticyclonic (at $f > 0$) or cyclonic (at $f < 0$) leeward eddy is formed behind the cape and remains there during whole modeling period, i.e. the eddy shedding mode is not realized. This situation is presented in Fig. 2 which corresponds to a run with following parameters: $D = 20$km, $|f| = 3\ 10^{-4}\mathrm{s}^{-1}$, $R_{bc} = 3.56$km, $\mathrm{Bu} = 0.032$, $U = 0.25$ and 0.27m/s, $\mathrm{Ro} = 0.042$ и 0.045 for the anticyclone and cyclone, respectively.

The eddy shedding mode at moderate values of Burger and Kibel-Rossby numbers, $0.2 < \mathrm{Bu} < 2.0$ and $0.15 < \mathrm{Ro} < 0.6$, is illustrated in Fig. 3, where $D = 15$km, $|f| = 1\ 10^{-4}\mathrm{s}^{-1}$, $R_{bc} = 10.7$km, $\mathrm{Bu} = 0.50$, $U = 0.35$ and 0.48m/s, $\mathrm{Ro} = 0.23$ and 0.32 for the anticyclone and cyclone, respectively.

When the Burger and Kibel-Rossby numbers become as large as $2 < \mathrm{Bu} < 8$ and $0.4–0.6 < \mathrm{Ro} < 1.4$, the eddy shedding does not stop but the eddies weaken (the rotation velocities become smaller than the longshore flow velocity) and stretch along the shoreline. Finally, at large Burger and Kibel-Rossby numbers, $\mathrm{Bu} > 8$ and $\mathrm{Ro} > 1.4$ the leeward eddies do not formed at all, and the longshore flow, being separated from the shoreline just behind the cape, smoothly approaches back to the shoreline at the distance of about $10D$ downstream (see Fig. 4a).

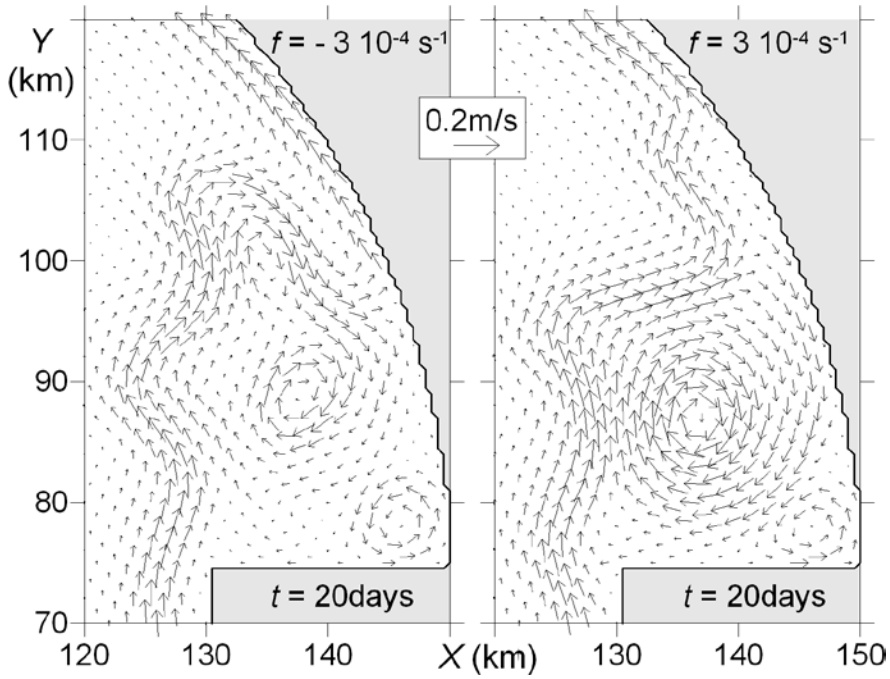

Fig. 2. Simulated surface layer velocity past the cape-like obstacle at t=20 days and following governing parameters: D=20km, $|f|=3\ 10^{-4}s^{-1}$, R_{bc}=3.56km, Bu=0.032, U=0.25 and 0.27m/s, Ro=0.042 and 0.045 for anticyclone and cyclone, respectively. The figure illustrates the trapped leeward eddy mode at Bu<0.2 and Ro<0.6.

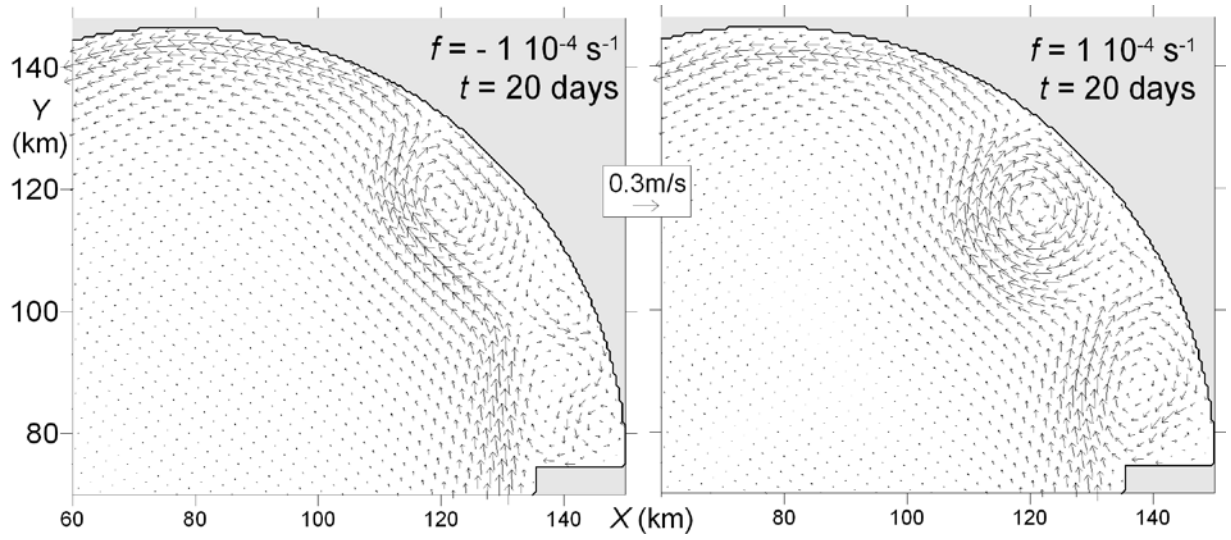

Fig. 3. The same as in Fig. 2 but for D=15km, $|f|=1\ 10^{-4}s^{-1}$, R_{bc}=10.69km, Bu=0.5, U=0.35 and 0.48m/s, Ro=0.23 and 0.32 for anticyclone and cyclone, respectively. The figure illustrates the shedding leeward eddy mode at Bu>0.2 and Ro<0.6.

Since in the main body of numerical experiments, performed with varying of *D* and *f*, the no leeward eddy mode realized at simultaneous increase of both Bu and Ro, it remained unclear the increase of which parameter, Bu or Ro, was responsible for the leeward eddy disappearance. To make the issue clear, the numerical experiments with large Burger and Kibel-Rossby numbers, $\mathrm{Bu} > 2$ and $\mathrm{Ro} > 0.6$, were reproduced at the same values of *D*, *f*, and other parameters, but smaller τ_0 from the range of $\tau_0 = 0.0125$–$0.1\mathrm{N/m}^2$, which conserved the old values of Bu but decreased Ro (due to the decrease of *U*). Achieved in this way decrease of the Kibel-Rossby number to $\mathrm{Ro} < 0.6$ was found to be enough to restore the leeward eddy shedding mode in all numerical experiments with large Burger number $\mathrm{Bu} > 2$. Comparison of Fig. 4, a and b, displays the transition from the no leeward eddy mode to the leeward eddy shedding mode with the decrease of flow velocity *U*.

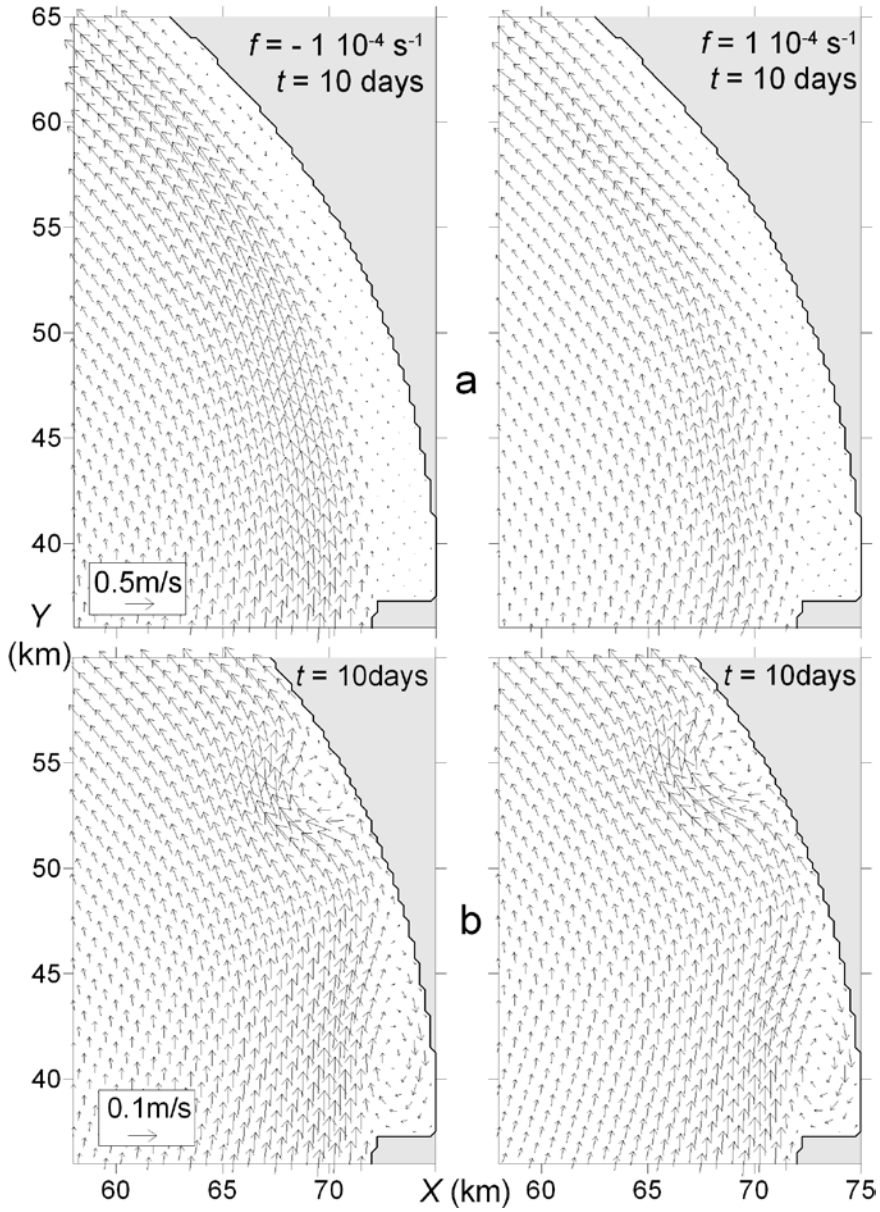

Fig. 4. a is the same as in Fig. 2, but for t=10days, D=3km, $|f|=1\ 10^{-4}\ s^{-1}$, R_{bc}=10.7km, Bu=12.7, U=0.47 and 0.57m/s, Ro=1.57 and 1.90 at f>0 and f<0, respectively. b is the same as a, but for smaller flow velocity, U=0.17 and 0.16 m/s, Ro=0.57 and 0.53 at f>0 and f<0, respectively.

The results of the above-described numerical experiments on leeward eddying past the cape-like obstacle in rotating stratified environment are generalized in Fig. 5 where a flow-mode diagram on the $(\mathrm{Ro}, \mathrm{Bu})$ plane is presented.

IV. Discussion and Conclusions

It follows from the comparison of the results of the laboratory experiments [2, 5] and our numerical experiments, that the way the flow past a coastal obstacle is produced can result in a substantial change of the leeward eddying regimes. If the flow past obstacle in rotating stratified channel is imitated by translating the channel floor, to which the obstacle is fixed [2], or by a change of the angular velocity of a round basin rotation provided that before the change the solid-body rotation state of fluid in the basin has been achieved [5], the effect of bottom friction

on leeward eddy formation, as applied to stratified environment, will be exaggerated to some extent. The cause is the vertically uniform flow generated in this way regardless of the presence of density stratification in the water column. The convergence/divergence of the bottom layer Ekman transport in the leeward eddy underneath can largely modify eddy's behavior and, at $\mathrm{Ro} = \mathrm{O}(1)$, result in an asymmetry of the wake dynamics with respect to cyclonic and anticyclonic eddies [5]. To the contrary, in our numerical experiments the flow past obstacle being generated by transient longshore windstress is substantially baroclinic: the flow velocity largely decreases with depth in the pycnocline layer which makes the bottom friction inessential. Note that there is a paired internal Ekman layer at the density interface, but the total, vertically-integrated Ekman transport through it is nil.

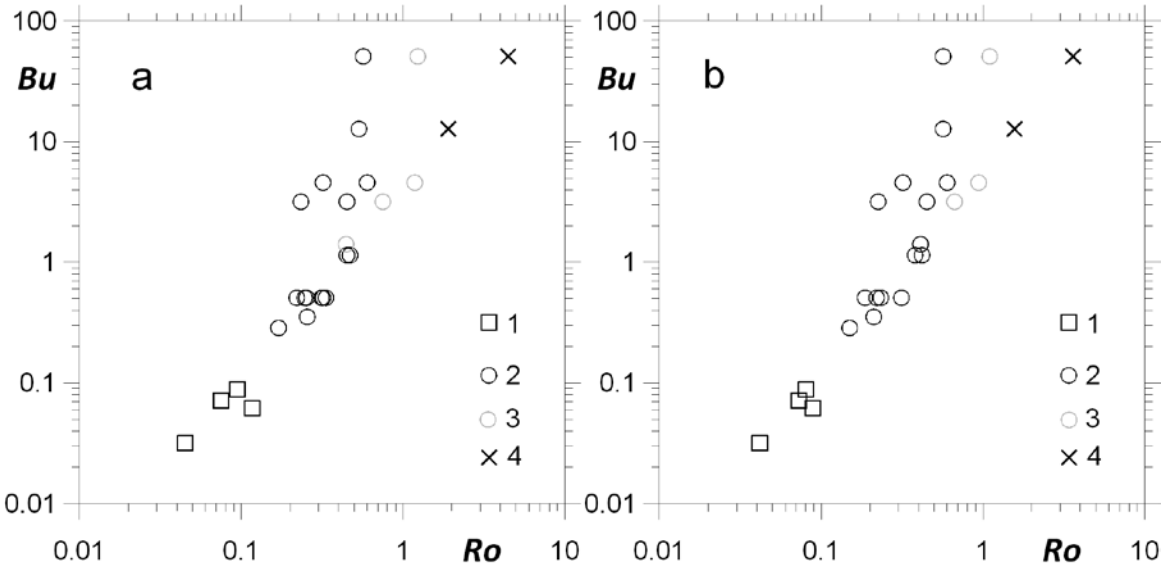

Fig. 5. A flow-mode diagram on the (Ro, Bu) plane plotted using results of all numerical experiments performed. The panels a and b relate to cyclonic and anticyclonic eddies, respectively. 1 – the trapped eddy mode, 2 – the eddy shedding mode, 3 – the weak elongated eddies, and 4 – separation of flow in the no leeward eddy mode.

Our numerical experiments showed that for moderate Kibel-Rossby number $\mathrm{Ro} < 0.6$, the leeward eddying mode depends on the value of Burger number: the trapped eddy mode at $\mathrm{Bu} < 0.2$ changed for the eddy shedding mode at $\mathrm{Bu} > 0.2$. This result is qualitatively similar to that of Boyer and Tao [2] who reported on the marginal value of $\mathrm{Bu} = 0.5$ for transition from the trapped eddy mode to the eddy shedding mode. The transition from the leeward eddy modes, either shedding or trapped, to the no leeward eddy mode with the increase of Kibel-Rossby number to $\mathrm{Ro} > 1.4$ could not be detected in [2, 5], because those laboratory experiments were performed at $\mathrm{Ro} < 0.6$. For this reason, the no leeward eddy mode at $\mathrm{Ro} > 1.4$ detected in our numerical experiments is believed to be a new finding. As to the marginal range of Kibel-Rossby number, $0.6 > \mathrm{Ro} > 1.4$, it is characterized by a weakening of leeward eddies and their stretching along the shoreline.

The weakening and ultimate cease of leeward eddying past a coastal cape-like obstacle in rotating stratified environment with the increase of $\mathrm{Ro} = U / |fD|$ to the value of the order of unity and larger can be qualitatively explained by the decrease of advection period, D/U, below the rotation period, $1/f$, so the liquid parcel can leave the past-cape wake zone before the

baroclinic eddy is formed. In a similar way, the transition from the eddy shedding mode to the trapped eddy mode with the decrease of $\mathrm{Bu} = (R_{bc} / D)^2$ to $\mathrm{Bu} < 0.2$ can be qualitatively explained by the fact that the typical size of baroclinic eddy, estimated though the wave length of the fastest growing mode of baroclinic instability as $4.9\, R_{bc}$ [8], becomes smaller than the wake zone width past the obstacle, *D*.

V. Acknowledgement

This work was supported by the Russian Science Foundation (Project No 14-17-00382). The authors thank A.G. Zatsepin and P.O. Zavialov for fruitful discussion.

VI. References

[1] A.F. Blumberg and G.L. Mellor, "Diagnostic and prognostic numerical calculation studies of the South Atlantic Bight," *J. Geophys. Res.*, vol. 88(C8), pp. 4579–4592, 1983.

[2] D. Boyer and L. Tao, "On the motion of linearly stratified rotating fluids past capes," *J. Fluid Mech*, vol. 180, pp. 429–449, 1987.

[3] P.A. Davies, P. Besley, and D.L. Boyer, "An experimental study of flow past a triangular cape in a linearly stratified fluid," *Dyn. Atmos. Oceans*, vol. 14, pp. 497–528, 1990.

[4] C. Dong, J.C. McWilliams, and A.F. Shchepetkin, "Island wakes in deep water," *J. Phys. Oceanogr.*, vol. 37, pp. 962–981, 2007.

[5] D.N. Elkin and A.G. Zatsepin, "Laboratory investigation of the mechanism of the periodic eddy formation behind capes in a coastal sea," *Oceanology*, vol. 53, pp. 24–35, 2013.

[6] P.K. Kundu and I.M. Cohen, *Fluid Mechanics*, 2nd ed., Academic Press, New York, 2002, 766 p.

[7] M.G. Magaldi, T.M. Özgökmen, A. Griffa, E.P. Chassignet, M. Iskandarani, and H. Peters, "Turbulent flow regimes behind a coastal cape in a stratified and rotating environment," *Ocean Modelling*, vol. 25, pp. 65–82, 2008.

[8] N. A. Phillips, "Energy transformations and meridional circulations associated with simple baroclinic waves in a two-level, quasi-geostrophic model," *Tellus*, vol. 6, pp. 273–286, 1954.

[9] R.D. Pingree and L. Maddock, "The effects of bottom friction and Earth's rotation on an island's wake," *J. Mar. Biol. Ass. UK*, vol. 60, pp. 499–508, 1980.

[10] E. Wolanski, J. Imberger, and M. Heron, "Island wakes in shallow coastal waters," *J. Geophys. Res.*, vol. 89(C6), pp. 10553–10569, 1984.

[11] V. Zhurbas, I.S. Oh, and T. Park, "Formation and decay of a longshore baroclinic jet associated with transient coastal upwelling and downwelling: A numerical study with applications to the Baltic Sea," *J. Geophys. Res.*, vol. 111(C4), doi:10.1029/2005JC003079, 2006.